

## CHARACTERIZATION OF COMPONENTS DYNAMIC BEHAVIOR IN AN INDUSTRIAL PNEUMATIC ACTUATION SYSTEM FOR UNCONVENTIONAL APPLICATIONS

**Marília Maurell Assad**

**Mauro Speranza Neto**

Pontifícia Universidade Católica do Rio de Janeiro, Mechanical Engineering Department,  
Rua Marquês de São Vicente, 225 - CEP 22453-900 - Gávea, Rio de Janeiro, RJ, Brazil  
marilia.assad@gmail.com; msn@puc-rio.br

**Marco Antônio Meggiolaro**

Pontifícia Universidade Católica do Rio de Janeiro, Mechanical Engineering Department,  
Rua Marquês de São Vicente, 225 - CEP 22453-900 - Gávea, Rio de Janeiro, RJ, Brazil  
meggi@puc-rio.br

**Abstract.** *Pneumatic equipment is lightweight, cheap, clean and low-risk, being suitable for applications that require strength and high responsiveness. Nevertheless, this type of system has some limitations due to the air main feature: its compressibility results in nonlinear effects in the system, from the turbulent flow control valves to its performance inside the cylinder - which includes high sensitivity to friction and dead volumes during the stroke piston. These particular characteristics make its control and precise positioning difficult, limiting its application, especially when considered its use in a mechanism such as a Stewart Platform in a reduced scale. The present paper presents the modeling, computational simulation and experimental analysis of the dynamic behavior of a pneumatic actuation system that includes an unconventional flow control valve, consisting of four proportional valves, and a double acting single rod actuator. The final goal of this work is to, based on experimental results, determine the characteristics of these components in order to develop real-time control strategies which can minimize the effects of those typical nonlinearities for their use in the mechanism mentioned above.*

**Keywords:** *Pneumatic actuation systems, experimental modeling, unconventional control valve*

### 1. INTRODUCTION

Pneumatic actuators exhibit highly nonlinear characteristics due to the compressibility of its main feature: air. The effects of the gas in the system consist mainly of turbulent flows and losses through the control valves, delay and attenuation of flow rate through the pipe connection system - which in industrial environments tend to be even more significant due to the larger distance among the components of system operation - culminating in a high sensitivity to friction and the effect of capacitance in the volume of air inside the chambers, which can be compressed or expanded with the movement of the rod.

This paper aims to experimentally obtain the parameters of the dynamic model of the actuation system, based on the individual analytic model of each of its components. Model validation is then carried out through comparing experiment and simulation results. Afterwards, the model can be used to design control strategies to minimize the nonlinear effects in this type of system and optimize its positioning and tracking performance.

The isentropic thermodynamic process is the most widely used model to represent the pressure change inside the pneumatic cylinder's chambers. In this model, the ratio of specific heats is considered constant and the process, adiabatic and reversible, as can be verified in the work of Endler et al., (2008), Krivts and Krejnin (2006) and Perondi (2002). The polytropic process is considered by a few authors, such as Beater (2007) and Richer and Hurmuzlu (2001), where the ratio of specific heats varies from one to the admissible value in the isentropic process.

The turbulent and compressible flow through the variable area orifices of the control valve was modeled according to the traditional fluid flow presented on Fox et al., (2006), though some authors, such as Ning and Bone (2005), prefer to develop an experimental model to this component. Recent work (Andrighetto et al., 2006) has experimentally proved the efficiency of the Stribeck-Coulomb friction model in pneumatic actuators, which was proposed by Nouri et al., (2000) and is the most realistic friction model amongst the classic concept of static and dynamic friction.

The pipeline is rarely modeled in pneumatic systems, since its effects are only clearly perceived in long lines, over a meter long. Beater (2007) demonstrates some classical and empirical models to friction in long tubes; Richer and Hurmuzlu (2001) propose a model based on a wave equation in one dimension with dissipative terms.

## 2. PNEUMATIC SYSTEM

In order to validate and adjust the proposed models, a test rig was built (Fig. 1). The equipment was constructed to reproduce the typical movements of a simulator such as a Stewart platform. It has mechanical supports and its pneumatic connections are easily plugged, which allows various settings to position its elements, in order to study each nonlinearity isolated.

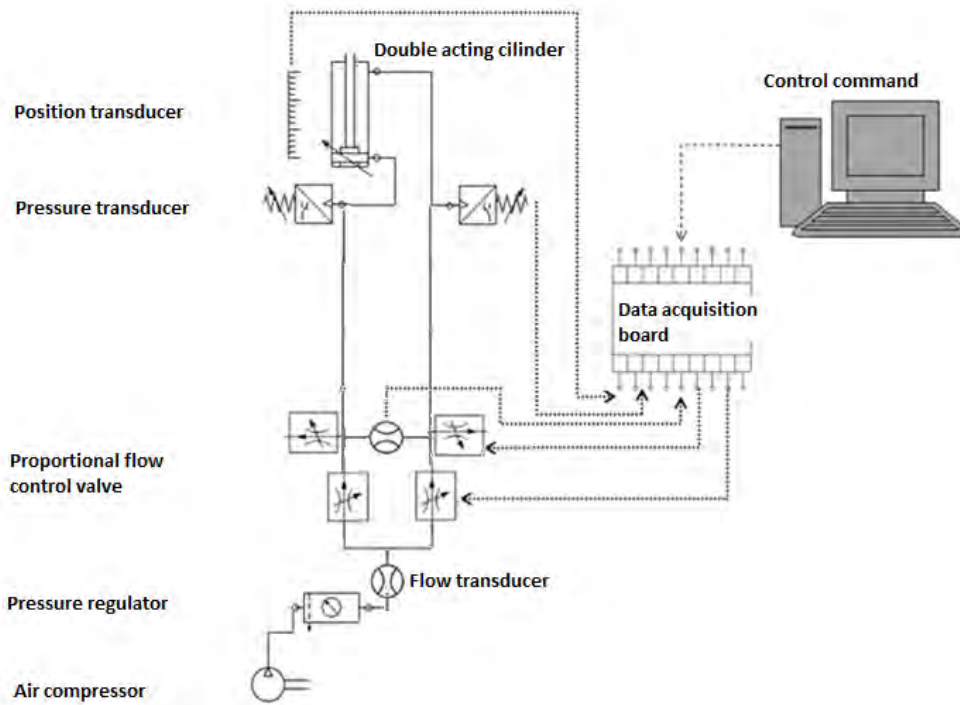


Figure 1. Test rig.

The test rig consists of: a compressor and a pressure regulating valve, two flow transducers, three pressure transducers, one position transducer coupled to a double actuated pneumatic cylinder and an unconventional servovalve assembly. The data acquisition system consists of two analog cards from National Instruments connected in parallel and serial communication with a computer.

Table 1. Experimental system components' specification.

Cylinder	Model	C85N16-50/SMC
	Length of the cylinder	50 mm
	Bore size (diameter)	16 mm
	Rod size (diameter)	6 mm
Supply pressure	5 bar	
Proportional flow control valve	Model	PVQ13-6L-03-M5-A/SMC
	Flow capacity	5 l/min

Regarding the set of servovalves, since a bidirectional flow control valve could not be found in the desired proportions and capacity, a combination of proportional valves was built to behave as that one. Thus, for each chamber of the actuator, proportional valves allow or block the passage of air and also control flow rate. In other words, these valves control the starting, stopping and direction of actuator motion while also controlling the speed at which it occurs.

Some considerations were made to simplify the model in order to facilitate its numerical simulation and control design, such as:

- The air behaves as an ideal gas.
- All processes are adiabatic, without heat transfer between the components and the environment.
- The specific heat at constant pressure and volume do not change during the process.
- The kinetic energy of the gas is neglected.

Next, the procedures for obtaining the mathematical models of the three main elements of the system, the pneumatic actuator, pipeline and control valve, are detailed.

## 2.1 Flow rate through control valve

The flow control valve is the main control element in the system: through electrical signals it is possible to vary the speed and direction of air flow to the pneumatic actuator. However, since this control is accomplished by varying the area of its orifice, it results in load loss effects and throttling due to the compressibility of gas. Assuming the flow rate is modified only by the area variation, there is no heat transfer, shock or friction in the passage of gas, characterizing a reversible and adiabatic flow, that is, an isentropic flow. It is further assumed that the velocity is constant and the flow rate, unidirectional.

Under these conditions, the flow rate will depend on the ratio between the pressures upstream and downstream. If the flow rate is larger than a critical value  $p_{cr}$ , the flow rate will depend directly on a nonlinear relationship between the two pressures. Otherwise, the flow attains a choked condition, at which it depends linearly on the upstream pressure. Considering a constant supply and exhaust pressure and according to the standard orifice theory from Fox et al. (2006), the mass flow rate through the valve orifice takes the form:

$$q_m = \begin{cases} C_d A_o(x_v) C_1 \frac{p_u}{\sqrt{T}} & \text{if } \frac{p_d}{p_u} \leq p_{cr} \\ C_d A_o(x_v) C_2 \frac{p_u}{\sqrt{T}} \frac{p_d}{p_u} \sqrt{1 - \left(\frac{p_d}{p_u}\right)^{(k-1)/k}} & \text{if } \frac{p_d}{p_u} > p_{cr} \end{cases} \quad (1)$$

Being  $q_m$  the mass flow rate through the orifice considered;  $C_d$  the discharge coefficient, a dimensionless variable;  $A_o$  the orifice cross-sectional area, variable according to the control signal  $x_v$  given to the servovalve;  $T$  the temperature and  $p_d$  and  $p_u$ , respectively, the pressures downstream and upstream the flow. Also:

$$C_1 = \sqrt{\frac{k}{R} \left(\frac{2}{k+1}\right)^{\frac{k+1}{k-1}}} \quad C_2 = \sqrt{\frac{2k}{R(k-1)}} \quad p_{cr} = \left(\frac{2}{k+1}\right)^{\frac{k}{k-1}} \quad (2)$$

For air, the ratio of specific heat ratio ( $k$ ) is equal to 1.4, resulting in  $C_1 = 0.0404$ ,  $C_2 = 0.1562$  and  $p_{cr} = 0.528$ ;  $R$  is the ideal gas constant. The model also takes into account the direction of flow: for a charging process, the upstream pressure is the one coming from the compressor, and the pressure downstream is the one in the chamber; for discharging process, the upstream pressure becomes the atmospheric pressure and the pressure in the chamber is the downstream pressure.

Tests were carried out to determine the parameters of the experimental curve between the mass flow rate and the control signal applied to the valve (Fig. 2). The proportional valve was connected to the compressor and the atmosphere, with a pair of pressure and flow transducers before and after it; since the flow transducers measure volumetric flow rate, it is necessary to multiple its data by the air density, considered constant and equal to 1.178 kg/m<sup>3</sup>.

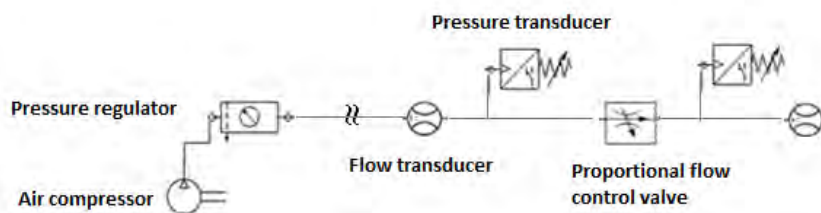


Figure 2. Valve test.

Since the downstream and upstream pressures are constant and known, the only unknown variables are the discharge coefficient and the orifice cross-sectional area. Thus, it was decided to determine a function,  $K_{vp}$ , which includes the dependence of both the discharge coefficient and the area change with control signal.

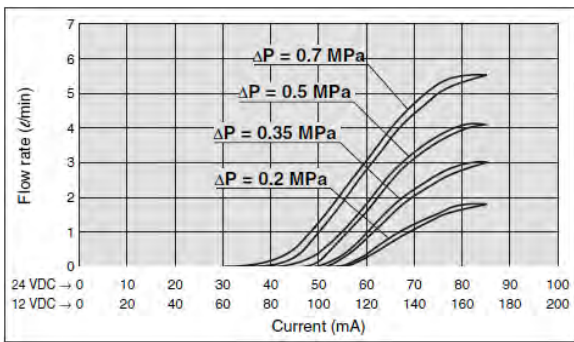
Equation 3 provides the best interpolation of function  $K_{vp}$  and Eq. 4 summarizes the new flow rate model – with  $C_1$ ,  $C_2$ ,  $p_{cr}$  previously defined in Eq. 2 – with an adjustment term. Figure 3 brings the final result and a comparison between the manufacturer's expected behavior and the experimental performance.

$$K_{vp} = \begin{cases} q_{max} [a x_v^4 + b x_v^3 + c x_v^2 + d x_v] & \text{if } x_v < 0.75 \\ q_{max} & \text{if } x_v \geq 0.75 \end{cases} \quad (3)$$

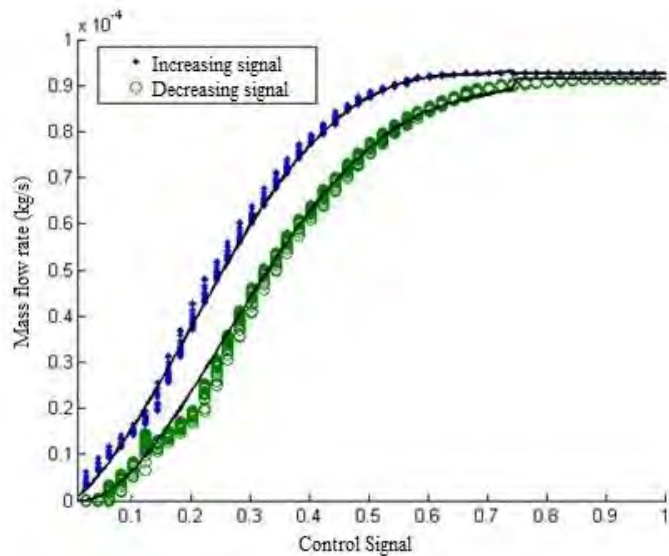
Table 2. Proportional valve model coefficients.

	a	b	c	d	max
Increasing current	10,93	-18,95	8,52	1,00	$9,25 \cdot 10^{-5}$
Decreasing current	9,86	-19,30	10,95	-0,21	$9,15 \cdot 10^{-5}$

$$q_m = \begin{cases} K_{vp}(x_v) \frac{C_1 p_u}{1181 \sqrt{T}} & \text{if } \frac{p_d}{p_u} \leq P_{cr} \\ K_{vp}(x_v) \frac{C_2 p_u}{1181 \sqrt{T}} \left(\frac{p_d}{p_u}\right)^{1/k} \sqrt{1 - \left(\frac{p_d}{p_u}\right)^{(k-1)/k}} & \text{if } \frac{p_d}{p_u} > P_{cr} \end{cases} \quad (4)$$



(a) Manufacturer's curve



(b) Experimental curve

Figure 3. Valve results.

To simplify the simulation and given that the two modeled curves are very close, it was chosen the increasing signal curve to characterize this element.

## 2.2 Flow rate through pipeline

The pipeline introduces two nonlinear effects to the pneumatic actuation system: a pressure drop along the tube; time delay and flow rate attenuation due to the travelling of the air wave through the line. To study both effects, one proportional valve was connected to a variable length pipeline along with a pair of flow and pressure sensors at the beginning and end of the tube. The result (Fig 4) is a system without influence from the actuator nonlinear effects and, since the components were horizontally placed, any gravitational effect on the air flow could be neglected. The pipeline length varied between 9 and 120 cm and the flow rate, between 0 and  $10^{-4}$  kg/s.

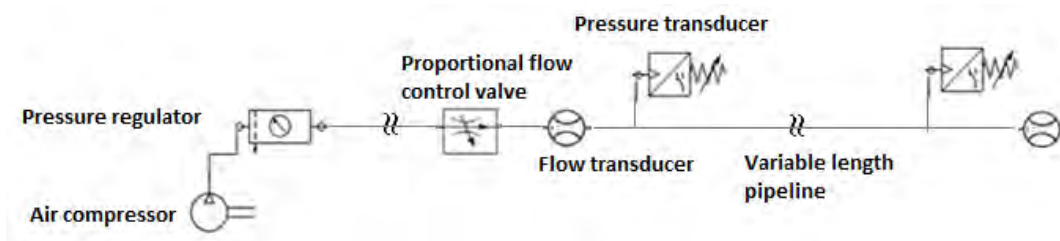


Figure 4. Pipeline test.

Maintaining the flow rate constant, the difference between the measurements obtained from the pressure transducer at the beginning of the tube and the one at the end gives the pressure drop along the hose. As can be verified by experimental results shown in Fig. 5, the maximum pressure drop on the line length commonly used (38 cm) was

around 1kPa, which represents 1% of atmospheric pressure. Thus, this effect can be neglected for the system under consideration.

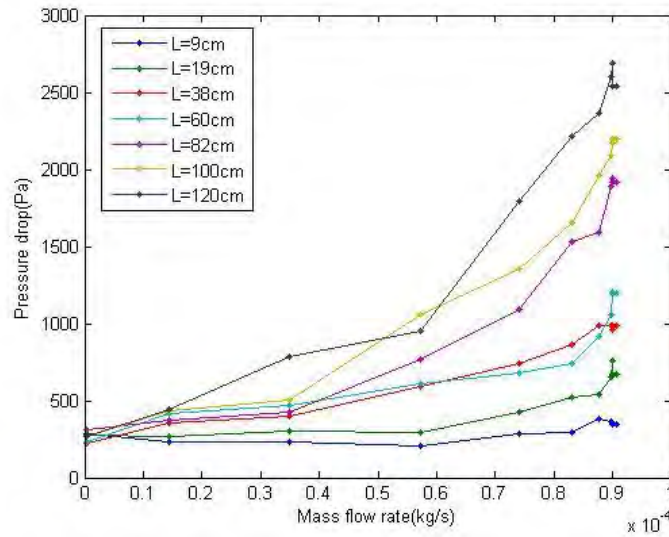


Figure 5. Pressure drop in pipelines of different length.

To determine the flow rate attenuation and time delay, only the maximum mass flow rate was analyzed. The comparison between the flow rate at the start and end of four pipelines lengths lies on Fig. 6. It can be concluded that the attenuation effect is negligible, since both transducers accuse similar flow rates.

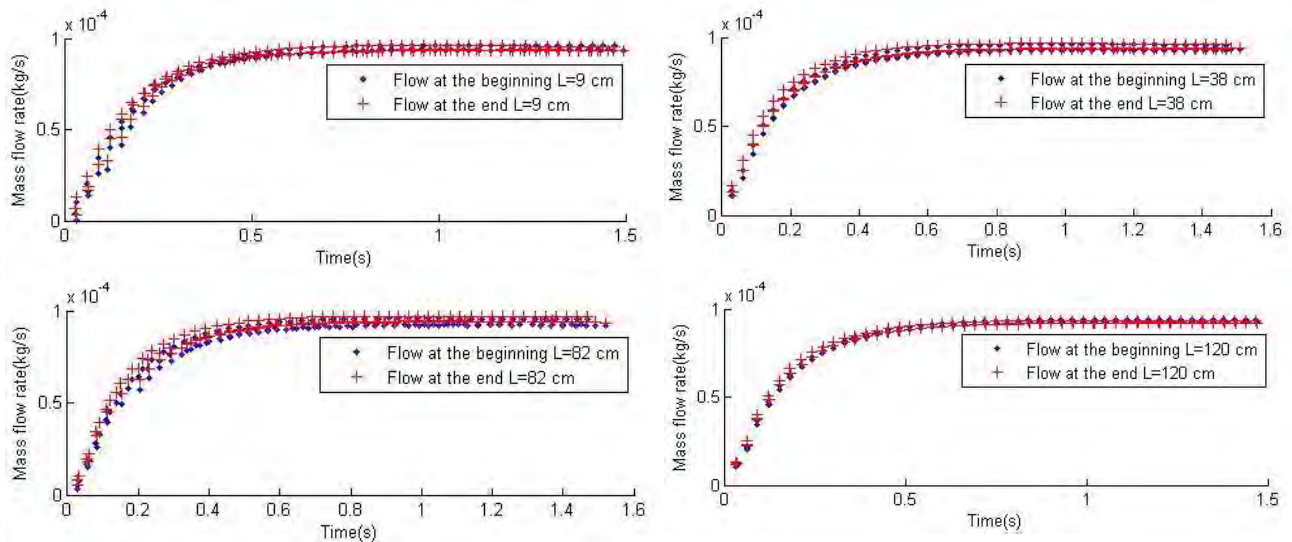


Figure 6. Flow rate attenuation and time delay.

Nevertheless, time delay is considerable in this component because it takes almost 0.5 second for the flow rate to reach the maximum value under a constant control signal on the proportional valve; therefore, an exponential function was modeled to represent this effect (Eq. 5 and Fig. 7).

$$q_m' = q_m (1 - e^{-\delta t}) \tag{5}$$

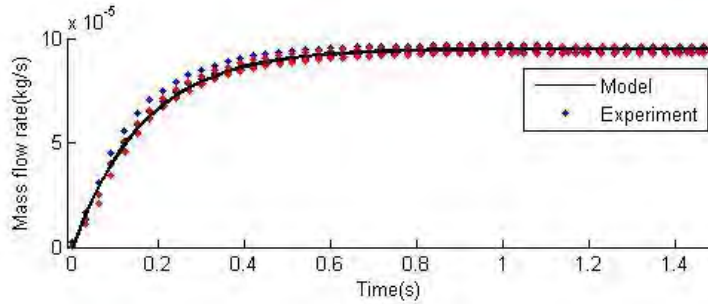


Figure 7. Time delay model.

### 2.3 Pressure in the chambers

The actuator chambers can be considered control volumes where there is fluid passage and the compression or expansion of air due to displacement of the piston. They can be modeled based on the principle of mass conservation, under some assumptions, such as: the pressure is uniformly distributed inside the chambers, the process is isentropic and the air is considered an ideal gas.

According to Fox et al. (2006), the rate of mass accumulation within the control volume must be equal to the difference between the mass flow rate entering and exiting this volume. Being  $q_m$  this difference:

$$q_m = \frac{\partial}{\partial t}(\rho V) = \rho \dot{V} + \dot{\rho} V \quad (6)$$

Being  $\rho$  the air density and  $V$  the air volume inside the chamber. The first term of Eq. 6 represents the mass accumulation rate due to fluid flow in the control volume and the second term represents gas compressibility. Since the process is considered isentropic and the air, an ideal gas, air density can be written as  $\rho = p/(RT)$ , being  $p$  the pressure in the chamber,  $R$  the universal gas constant and  $T$  the air supply temperature. That gives:

$$q_m = \frac{p}{RT} \dot{V} + \frac{\dot{p}}{kRT} V \quad (7)$$

With  $k$  being the ratio between the specific heat values at constant pressure and constant volume, as  $k = C_p/C_v$ . Considering the origin of the rod displacement in the middle of the cylinder stroke, Eq. 7 results in:

$$\begin{aligned} \dot{p}_1 &= \frac{kRT}{V_{01} + A_1(L/2 + x)} q_{m1} - \frac{k A_1}{V_{01} + A_1(L/2 + x)} p_1 \dot{x} \\ \dot{p}_2 &= \frac{kRT}{V_{02} + A_2(L/2 - x)} q_{m2} + \frac{k A_2}{V_{02} + A_2(L/2 - x)} p_2 \dot{x} \end{aligned} \quad (8)$$

$V_{0i}$  being the dead volume in the cylinder ends,  $A_i$  the cylinder chamber's cross-sectional area,  $L$  the actuator stroke and  $x$  its displacement.

### 2.4 Load dynamics

The force equilibrium in the assembly consisted of the pneumatic actuator and its additional load can be described by Newton's second law:

$$M\ddot{x} = p_1 A_1 - p_2 A_2 - p_{atm} A_h - F_{at} - Mg \quad (9)$$

Being  $M$  the mass of the external load and piston rod,  $F_{at}$  the frictional forces between the cylinder and the air, which will be detailed in the next item,  $p_1$  and  $p_2$  the absolute pressures in each chamber of the actuator,  $p_{atm}$  the absolute ambient pressure,  $A_1$  and  $A_2$  the effective areas in each chamber,  $A_h$  the cross-sectional area of the rod and  $g$  the gravitational acceleration, for when the piston is not on the horizontal position.



## 2.5 Friction

The friction force is also an important feature of the pneumatic actuator: considered the most complex nonlinearity to be correctly modeled, it impairs a precise control because it causes tracking errors and stick-slip phenomenon. The latter is characteristic in pneumatic systems, in which the cylinder switches between sliding, once it overcomes static friction with the gas, to sticking, since dynamic friction tends to have a lower value than static friction. This means that at each stop or change of movement direction, there is a different frictional force which cannot be neglected. In the long run, this distortion limits the limit cycles around a desired position and results in steady errors.

There are two known models that, together, can represent the friction in the system: the Coulomb friction and the viscous friction. The former can be divided into a static force when the speed of the body is zero, and a dynamic force, constant and of lesser magnitude, which opposes the body motion. The second model is proportional to velocity by a constant known as the viscous friction coefficient. Those models can be expressed as:

$$F_{Coulomb} = \begin{cases} F_s & \text{if } \dot{x} = 0 \\ F_D \text{sign}(\dot{x}) & \text{if } \dot{x} \neq 0 \end{cases} \quad (10)$$

$$F_{viscous} = b\dot{x} \quad (11)$$

Where  $F_S$  and  $F_D$  are the static and dynamic friction forces,  $b$  is the viscous friction coefficient and  $\dot{x}$  is the rod speed.

The union of these two models causes a discontinuity in the transition from the static to the dynamic model. In order to make this transition smoother enters into evidence an effect known as Stribeck friction: the friction force decays smoothly from the static friction with increasing speed until it reaches a speed limit at which the system enters the dynamic model.

In this work, the friction was modeled according to Nouri et al (2000) and Andriquetto et al (2006). The model takes into account the three frictions previously defined: the Coulomb, viscous and Stribeck friction. Equation 12 brings the junction of these elements in a function of the frictional force dependent on the speed:

$$F_{at} = F_D + b\dot{x} + (F_S - F_D) e^{-\left(\frac{\dot{x}}{\dot{x}_s}\right)^2} \quad (12)$$

Where  $\dot{x}_s$  is the Stribeck speed. Figure 8 represents the relationship between the friction force and the pneumatic actuator speed.

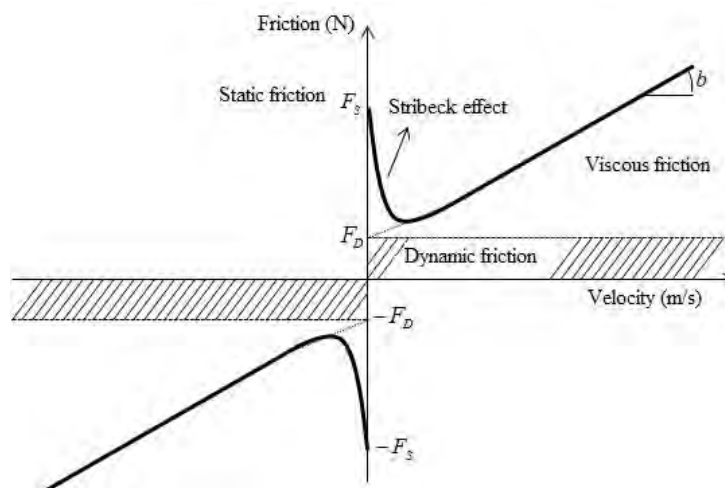


Figure 8. Friction force versus piston velocity.

Tests carried out to determine this parameter consisted in moving the piston in its full course with different velocities – obtained by varying the control signal to the servovalve – and analyzing the pressures inside the chambers and the actuator displacement. The control system maintains a constant signal to the valve until the actuator reaches its end; velocity and acceleration were obtained by numerical derivation of the displacement, avoiding the regions close to its limits. Friction force was then calculated according to Eq. 9. Experiments were made with the actuator in the horizontal and vertical position, with similar results (Fig. 9 and Tab. 3).

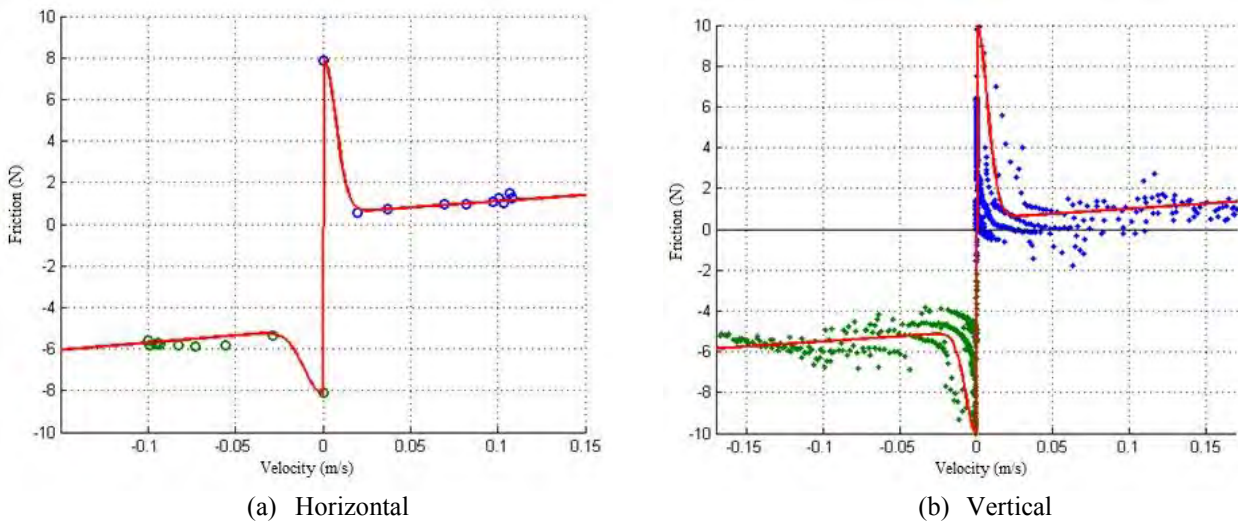


Figure 9. Experimental friction-velocity map.

Table 3. Friction model coefficients.

	Velocity	$F_S$	$F_D$	$b$	$\dot{x}_s$
Horizontal	Positive	8.0	0.5	6.0	0.01
	Negative	-8.1	-5.0	7.0	-0.01
Vertical	Positive	10	0.5	5.0	0.01
	Negative	-10	-5.0	5.0	-0.01

### 3. RESULTS

Model validation was conducted by comparing the open loop responses of the experimental system and simulation. Figure 10 brings the block diagram used to simulate the pneumatic system; each box has the individual model obtained for the control valve (Eq. 4), the pipeline (Eq.5) and the cylinder, which includes the pressure dynamic inside chambers (Eq. 8) and load dynamics with friction (Eq. 9 and Eq. 12).

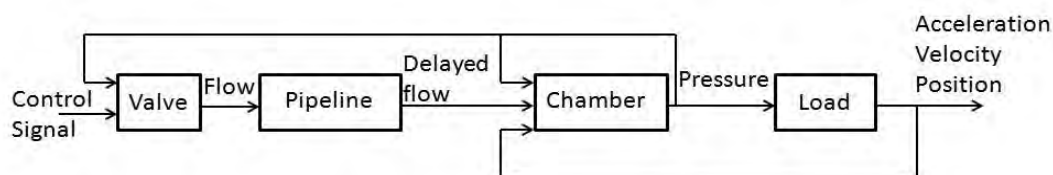


Figure 10. Simulation block diagram.

The parameters used in the experiments and simulations are:  $k = 1.4$ ,  $R = 287$  [J Kg/K],  $T = 293$  [K];  $x_v = \pm 1$  [V];  $A_1 = 2.01 \times 10^{-4}$  [m<sup>2</sup>],  $A_2 = 1.73 \times 10^{-4}$  [m<sup>2</sup>],  $V_{01} = 1.01 \times 10^{-7}$  [m<sup>3</sup>],  $V_{02} = 8.65 \times 10^{-8}$  [m<sup>3</sup>],  $p_{supply} = 5 \times 10^5$  [Pa],  $p_{atm} = 1 \times 10^5$  [Pa],  $L = 0.05$  [m], and  $M = 0.15$  [Kg].

Figure 11 illustrates the comparison between experiments and simulation results. The experimental tests were performed without an external load and with the piston in the vertical position. The system input was a step signal with maximum amplitude (1V) kept constant up until the actuator reaches 1 mm before the stroke limits – under these conditions, the mechanical stops are avoided. The tests were conducted with control signals of same value and opposite directions to each chamber, the same operating principle of a traditional bidirectional control valve. This means that when one chamber is being charged, the other one is being discharged.



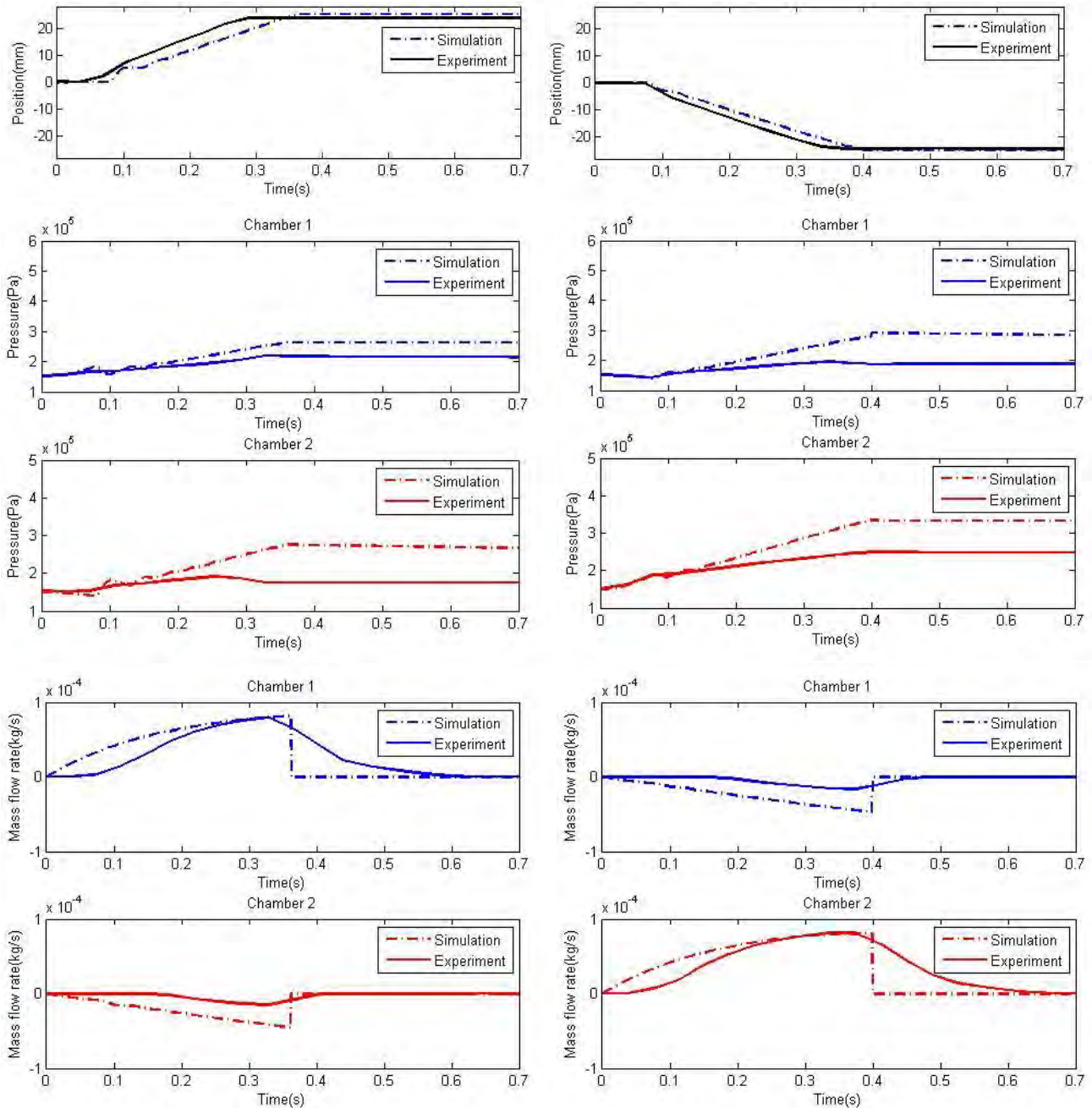


Figure 11. Simulation and experimental results.

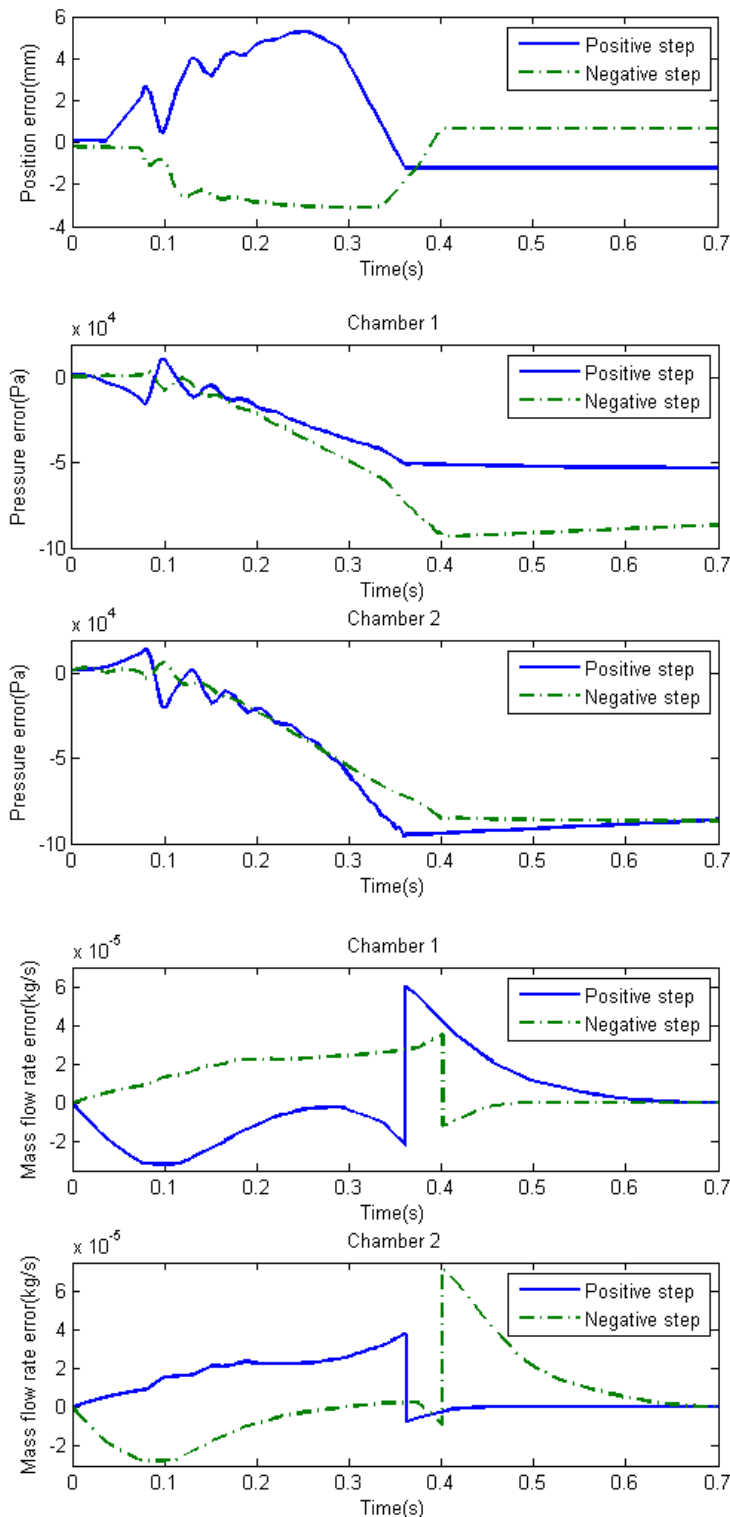


Figure 122. Differences between the experimental and simulated results.

It can be seen that the simulation performance agrees with the experimental results for the piston displacement, with errors up to 6mm. It is noticeable that the simulated chamber pressures are higher than those obtained from the experimental tests in the order of 0,1MPa – or 10% of the atmospheric pressure. That deviation is probably caused by cumulative numeric errors, since the pressure and flow rate are highly dependent.

As for the mass flow rate, the difference between the experimental and numerical results comes from programming issues. The theoretical flow rate model (Eq. 1) predicts instantaneous flow rates, either by minimally opening the valve

orifice or by totally closing it through control signals. On simulations, once the control signal is equal to zero, so it will be the flow area, resulting in an instantaneous null flow rate. In practice, this phenomenon cannot be reproduced because there is no instantaneous response. Furthermore, another factor that helps to increase this difference between experiment and simulation is the fact that the flow measurements were made by instruments that have some latency in their response, resulting in a smoother flow rate curve. Therefore, the simulations performance have demonstrated considerable errors in comparison with the experimental results.

#### 4. CONCLUSIONS

In this work, three components of an industrial pneumatic actuation system had its dynamic behavior individually characterized, along with its nonlinear effects: the nonlinear turbulent flow through the control servovalve; delayed flow through the pipeline; air compressibility and distinguished friction inside the cylinder's chambers. The nonlinear model of the pneumatic actuation system also takes into consideration the difference in effective areas on both sides of the piston, the inactive volumes at the ends of the stroke.

Experiments with the complete system and numerical simulations were carried out to prove the individual models' validity. A valid agreement was found regarding the displacement behavior, which proves the model suitability for future analysis, even though the pressure and mass flow rate has shown bigger differences in comparison with the experimental results.

As future works, the authors intend to use the nonlinear model to design control strategies in order to minimize the nonlinear effects in this type of system and optimize its positioning and tracking performance.

#### 5. ACKNOWLEDGEMENTS

This work had the financial support of Brazilian government organization CNPq (Conselho Nacional de Desenvolvimento Científico e Tecnológico).

#### 6. REFERENCES

- Andrighetto, P.L.; Valdiero, A.C.; Carlotto, L., 2006. *Study of the friction behavior in industrial pneumatic actuators*, In *ABCAM Symposium Series in Mechatronics*, Vol.2, pp 369-376.
- Beater, P. 2007. *Pneumatic drives – System design, modeling and control*, Springer.
- Endler, L.; Valdiero, A.C.; Andrighetto, P.L.; Marat, R., 2008. *Simulação computacional de um modelo matemático para atuadores pneumáticos*, In portuguese, In *TEMA (Tendências em Matemática Aplicada e Computacional)*, 9, No. 2.
- Fox, R.W; McDonald, A.T; Pritchard, P.J., 2006. *Introduction to fluid mechanics, 6<sup>th</sup> edition*, John Wiley & Sons.
- Krivts, I.; Krejnin, G., 2006. *Pneumatic actuating systems for automatic equipment –Structure and design*, Taylor&Francis.
- Ning, S.; Bone, G.M. 2005. *Development of a nonlinear dynamic model for a servo pneumatic positioning system* , In *Proceedings of the IEEE - International Conference on Mechatronics & Automation*, Niagara Falls, Canada
- Nouri, B., AI-Bender, F., Swevers, J., Vanherck, P. and Van Brussel, H., 2000. *Modeling a pneumatic servopositioning system with friction*. In *American Control Conference 2000*, pp. 1067-1071.
- Perondi, E.A. 2002. *Controle não linear em cascata de um servoposicionador pneumático com compensação de atrito*, In portuguese, Ph.D. Thesis, Department of Mechanical Engineering, Santa Catarina Federal University, Brazil.
- Richer, E.; Hurmuzlu, Y., 2000. *A high performance pneumatic force actuator system Part I – Nonlinear mathematical model*, In *ASME Journal of Dynamic Systems Measurement and Control*, Vol. 122, No.3, pp. 426-434.

#### 7. RESPONSIBILITY NOTICE

The authors are the only responsible for the printed material included in this paper.